

## Carbon Isotopic Evolution Characteristics and the Geological Significance of the Permian Carbonate Stratotype Section in the Northern Upper-Yangtze Region, Southern China

QU Hongjun<sup>1,\*</sup>, LI Peng<sup>1</sup>, LUO Tengwen<sup>1</sup>, GUAN Liqun<sup>1</sup>, FAN Yuhai<sup>2</sup> and WANG Li<sup>1</sup>

*1 State Key Laboratory of Continental Dynamics, Department of Geology, Northwest University, Xi'an 710069, China*

*2 Remote Sensing Application Institute of ARSC, Xi'an 710069, China*

**Abstract:** The Permian global mass extinction events and the eruption of the Emeishan flood basalts in the Upper Yangtze region should display certain responses during the evolution of carbon isotope. In this paper, the Permian carbon isotopic evolution in the Upper Yangtze region is examined through systematic stratotype section sampling and determination of <sup>13</sup>C in the northern Upper-Yangtze regions and Southern China. Additionally, the carbon isotopic evolution response characteristics of the geological events in the region are evaluated, comparing the sea-level changes in the Upper Yangtze region and the global sea-level change curves. Results of this study indicated that the carbon isotopic curves of the Permian in the Upper Yangtze region are characterized by higher background carbon-isotope baseline values, with three distinct negative excursions, which are located at the Middle–Late Permian boundary and the late period and end of the Late Permian. The three distinct negative excursions provide an insightful record of the global Permian mass extinction events and the eruption of the Emeishan flood basalts in the Upper Yangtze region. The first negative excursion at the Middle–Late Permian boundary reflected the eruption of the Emeishan flood basalts, a decrease in sea level, and biological extinction events of different genera in varying degrees. The second negative excursion in the Late Permian included a decrease in sea level and large-scale biological replacement events. The third negative excursion of the carbon isotope at the end of the Permian corresponded unusually to a rise rather than a decrease in sea level, and it revealed the largest biological mass extinction event in history.

**Key words:** carbon isotope, mass extinction, eruption of Emeishan Flood Basalts, Permian, the Upper Yangtze region

### 1 Introduction

In geological history, the carbon isotope composition is an important index for studying the biological events and environmental changes that occur over time. Many important events in the development and evolution of the earth are recorded that have the potential to affect global changes in sea level, greenhouse or icehouse climatic conditions, relative changes in the stocks of organic and inorganic carbon, and biological extinction or replacement (Guo Qingjun et al., 2006; Wang et al., 2009; Zeng et al., 2012; Wei, 2015; Liu Shuhua et al., 2016; Lan Yefang et al., 2016). Organic carbon isotopes in sediments have

frequently been used to identify the source of organic matter (Wu Libin et al., 2017; Wu Xiaoqi et al., 2017). Since the 1990s, significant progress has been made in the study of carbon isotopes in marine carbonate rocks. The change in carbon isotopic composition in carbonate rocks can reflect the organic carbon production in a paleo-ocean environment (Magaritz et al., 1988; Li Renwei et al., 1999; Zhu Jingquan, 2004; Cui et al., 2017). Previous studies on carbonate rocks have reconstructed the thermohaline circulation process of the paleo-ocean (Railsback et al., 1990; Wenzel et al., 1996). This research has suggested that the carbon–oxygen isotopic composition of carbonate rocks is closely related to paleoclimates and paleo-marine environments (Yan Zhaobin et al., 2005; Michael and Chris, 2006; Shen

\* Corresponding author. E-mail: hongjun@nwu.edu.cn

Shuzhong et al., 2010; Munnecke et al., 2010; Sanson-Barrera et al., 2015). Du et al. (1994) ascertained the relationship between carbon–oxygen isotopes and sea-level changes by studying the Upper Sinian-Ordovician carbon–oxygen isotopic sections in the Kalpin area of Xinjiang Province (Du Xiaodi et al., 1994). Huang et al. (2012) measured the carbon isotopes of marine carbonate rocks around the Permian–Triassic boundary in the Upper Yangtze area, which reflected the rapid biological declines and mass extinctions across the Permian–Triassic boundary (Huang Sijing et al., 2012; Xiao Sheng et al., 2015; Zhou Yexin et al., 2017).

The Permian is an important period for the formation, development, and evolution of the united ancient land in the world. There has been a series of major geological events, including a high frequency of drastic eustatic change in sea level (Haq and Schutter, 2008; Qiu et al., 2014), extensive glacier activity (Veevers and Powell, 1987; Isbell et al., 2003; Chen et al., 2013), severe volcanic activity, and biological extinctions (Wignall and Twitchett, 1996; Wang and Sugiyama, 2000; Cao Changqun et al., 2002; Payne et al., 2004; Korte et al., 2006; Peng et al., 2007; Isozaki et al., 2007a, b; Heydari, 2008; Wignall et al., 2009; Isozaki, 2009; Korte et al., 2010; Shen Shuzhong et al., 2010; Shen et al., 2011; Payne et al., 2011; Hermann et al., 2011; Liu et al., 2013; Burgess et al., 2014; Song et al., 2015; Zhang et al., 2015; Erwin, 2015; Qian Xin et al., 2016). The Emeishan flood basalts erupted in the Permian in the Upper Yangtze region (Zhou et al., 2002; Xu et al., 2004; Zhang Zhaochong et al., 2006; He et al., 2007; Luo Zhenyu et al., 2007; Xu Yigang et al., 2013; Shellnutt, 2014). Sea-level changes are controlled directly or indirectly by a series of geological events, such as orogenic movements, glacial activities, submarine expansions, and paleoclimates (Huang Sijing et al., 2001, 2005, 2008; Coogan and Dosso, 2015; Van der Meer et al., 2017; Godd eris et al., 2017). The carbonaceous isotopic composition and evolution of Permian seawater can record these geological events, and it is thus worth studying the response and evolution characteristics in the carbonaceous isotopic records.

Outcrops of stratigraphic Permian marine carbonate platforms were well developed in the northern part of the Upper Yangtze and continuous marine sediments have been recorded. In this paper, the carbon and oxygen isotopic evolution of the Permian in the Upper Yangtze region can be ascertained by the systematic sampling and determination of  $\delta^{13}\text{C}$  in stratotype sections of carbonate in the northern Upper Yangtze region. Moreover, a comparison of the relative sea-level changes in the Upper Yangtze region and the global sea-level change curves can

be indicative of the relationship between the response characteristics of Emeishan basalt eruptions and major biological extinction events to carbon and oxygen isotope evolution curves. Such a comparison can also reflect the response of carbon and oxygen isotope evolution associated with the above mentioned geological events in the Upper Yangtze region.

## 2 Geological Settings

Located in the northern margin of the Upper Yangtze Block, the Tongjiang area in Sichuan Province is located in the northeast part of the Sichuan Basin, in front of the Micangshan thrust belt, with the center-Sichuan gentle tectonic belt located to the south and the Dabashan arc-shaped thrust belt located to the northeast (Fig. 1).

The northern margin of the Upper Yangtze was adjacent to the Mianlue Ocean in Permian period (Fig. 2), and was the passive continental margin of the Mianlue Ocean (Dong et al., 2015; Dong and Santosh, 2016). During the initial Qixia stage (Early Permian), widespread marine transgression in the Yangtze region submerged the Yangtze plate, which resulted in the sedimentation of carbonate rocks as a stable platform in the Middle Permian. The transgression further expanded during the Maokou stage, forming an open carbonate platform, carbonate shelf-slope system, and epeiric sea-hemipelagic siliceous basin system from south to north, displaying a typical continental margin.

At the end of the Maokou stage, the Upper Yangtze region entered its peak of expansion, and the Emeishan earth-shaking movement reached a climax with large-scale eruptions of the Emeishan basalts (Zhou et al., 2002; Zhang Zhaochong et al., 2006; He et al., 2007; Wang Qingchen and Cai Liguang, 2007; Xu et al., 2008; Shellnutt et al., 2014). After the Dongwu movement, the ancient Mianlue Oceanic Basin of the Late Permian continued to expand. The initial transgression in the Wujiaping stage indicated that the scale of transgression was larger in the west and smaller in the east. Coal-bearing sedimentary deposits developed in the central and southern Sichuan area, which were represented by the Longtan Formation, while carbonate sediments of the Wujiaping Formation were extensively deposited in the eastern Sichuan area. The transgression coverage during the Changxing period expanded and the scope of the northern deep-water basin also expanded (Yang Yuqing and Feng Zengzhao, 2000).

The Permian in the northeastern Sichuan Basin from bottom to top consisted of the Middle Permian and the Upper Permian, while the Lower Permian was generally missing (Li Xia et al., 2005). The Middle Permian includes the Qixia and Maokou Formations, and the Upper

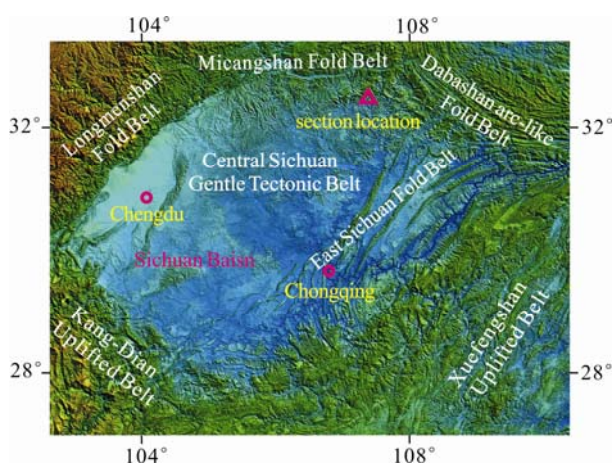


Fig. 1. Tectonic units of the study area and location map of the section.

Permian consists of the Wujiaping and Changxing Formations. The Permian is unconformably in direct contact with the underlying Silurian in unconformity, and is in contact with the overlying Triassic in conformity.

### 3 Section Lithology Characteristics, Samples, and Methodology

The Permian stratigraphic stratotype section is located in the Longhu Cave Scenic Area about 10 km north of Pingxi, Tongjiang County, Sichuan Province, China (Fig. 3a).

#### 3.1 Profile lithology and sedimentary characteristics

The Permian stratigraphic stratotype section of Longhu Cave consists of the Qixia, Maokou, Wujiaping, and

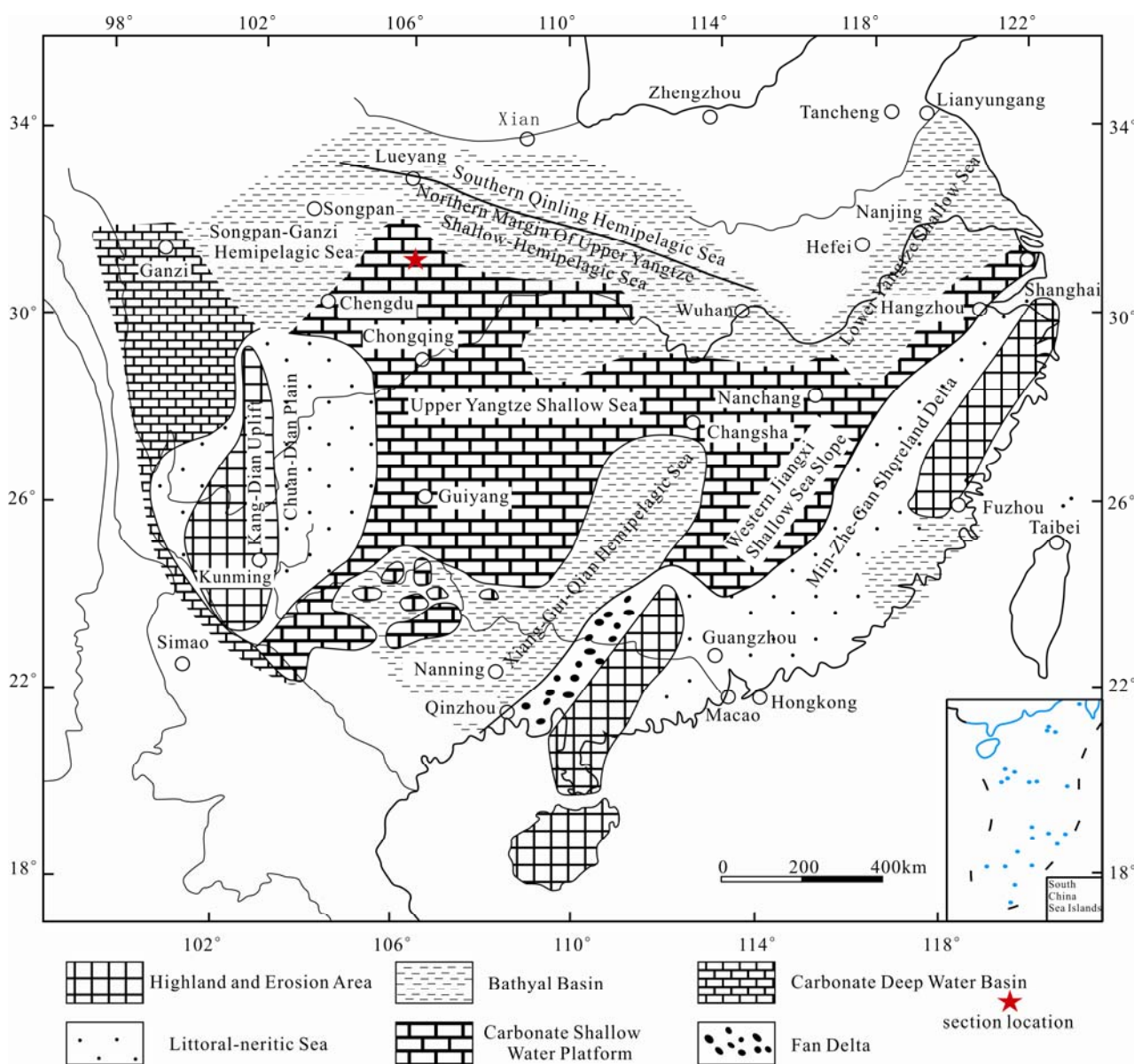


Fig. 2. Permian tectonic palaeogeographic map of South China and the section location (after Wang and Cai, 2007).

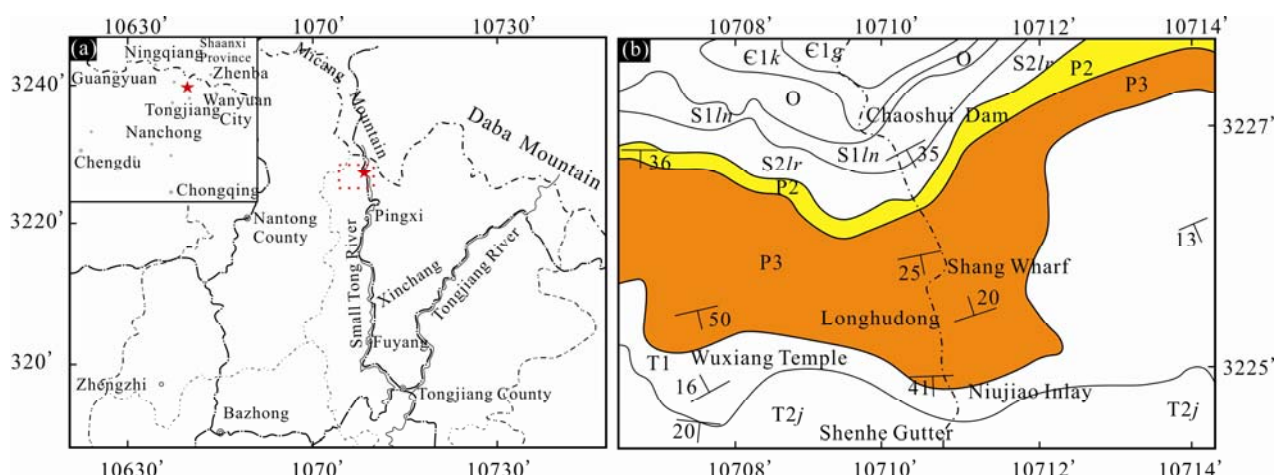


Fig. 3. Section location and geological sketch map of Longhu Cave section in the Tongjiang area, Sichuan Province, China.

(a), Section location of Longhu Cave Scenic Area in the Tongjiang area, Sichuan Province, China; (b), geological map of Longhu Cave Scenic Area in Tongjiang area.

Changxing Formations from bottom to top. The Permian is unconformably in contact with the underlying Silurian and is conformably in contact with the overlying Triassic (Fig. 3b). In addition to the lack of a bottom of the Qixia Formation and a short-term depositional discontinuity between the Maokou and Wujiaping Formations, the middle to Upper Permian are on the whole continuous marine sediments, with a total thickness of 1102.6 m, which is divided into 37 smaller layers (Fig. 4). The specific lithology and sedimentary characteristics of the section are as follows:

### 3.1.1 The Qixia Formation ( $P_{2q}$ )

The Qixia Formation is unconformably in contact with the underlying Silurian strata. It is generally composed of dark-gray bone debris limestones with mud-sized grain and micrites, with black-gray carbonaceous shales at the bottom and chert nodule at the top. It has pimple-shaped and augen structures, with fossilized small insects and corals, and it consists of carbonate platform facies deposition (Jin Yugan et al., 1999; Li Guohui et al., 2005).

### 3.1.2 The Maokou Formation ( $P_{2m}$ )

The Maokou Formation is conformable in contact with the underlying Qixia Formation. The lower part includes black-gray and dark-gray micrites with mud-sized grains, bone debris micrites with black calcareous shales, with a thin layer of siliceous rocks in the top section. The middle section consists of light-gray and dark-gray thick-layered bone debris micrites, bioclastic limestones, and micrites with chert nodules. The upper section includes light-gray micrites with chert nodules and bioclastic limestones, and it also consists of carbonate platform facies deposition (Wang Chengshan et al., 1999; Deng Hongying et al.,

1999; Li Guohui et al., 2005).

### 3.1.3 The Wujiaping Formation ( $P_{3w}$ )

The Wujiaping Formation is parallel unconformably in contact with the underlying Maokou Formation, whose bottom often developed the Wangpo shale member, the Wujiaping Formation has coal-bearing strata of marine-terrestrial facies. Which consist of variegated aluminous shales or claystones, with carbonaceous limestones, bauxites, coal lines, and lenticular limestones, including plant fossils. While this section missed the Wangpo shale member, the main body of the Wujiaping Formation includes gray, and light taupe-gray thick-layered massive micrites, limestones with calcareous, siliceous, and carbonaceous shales, mainly distributed to the northeast of Sichuan Province, it includes carbonate platform facies of the epicontinental sea (Jin Yugan et al., 1999; Li Guohui et al., 2005).

### 3.1.4 The Changxing Formation ( $P_{3c}$ )

The Changxing Formation is conformably in contact with the underlying Wujiaping Formation. The lower section consists of dark-gray thick micrites, bone debris limestones, and a small amount of black calcareous shales. The middle-upper section is a gray middle-thick layer containing chert nodules, zebra limestone and dolomite limestones. The top section includes steel-gray thin-layer micrites, interbeds of dolomite limestones and claystones in different thickness containing siliceous layers and flint strips, and it also consists of carbonate platform facies deposition (Jin Yugan et al., 1999; Li Guohui et al., 2005).

## 3.2 Sample collection

A total of 102 limestone samples were collected from bottom to top in the stratigraphic Permian section of

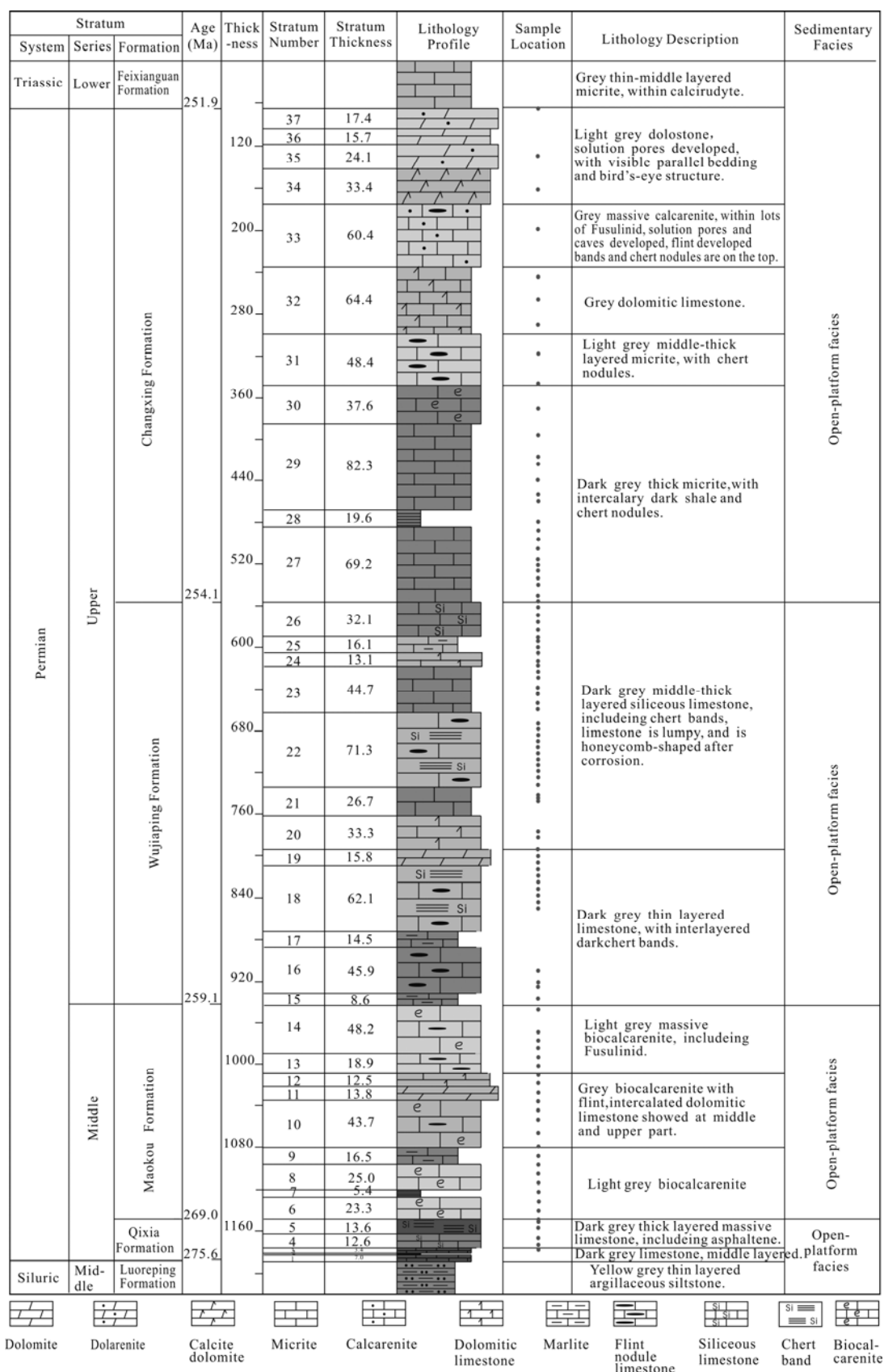


Fig. 4. Composite columnar map and sample locations of the Permian in the Tongjiang area, Sichuan Province, China.

**Table 1 Statistics of Permian samples in Tongjiang area, Sichuan province**

Formation	Number of layers	Thickness (m)	Number of samples	Sampling density (m)
Qixia Formation	5	38.70	6	6.4
Maokou Formation	9	207.3	22	9.4
Wujiaping Formation	12	372.6	47	8.1
Changxing Formation	11	472.5	27	17.5

Longhu Cave in Tongjiang, Sichuan Province with an average interval of 11.7 m (Table 1; Fig. 4). Among them, six samples are from the Qixia Formation with a total thickness of 38.7 meters, 22 samples are from the Maokou Formation with a total thickness of 207.3 meters, 47 samples are from the Wujiaping Formation with a total thickness of 372.6 meters, and 27 samples are from the Changxing Formation with a total thickness of 472.5 meters (Table 1).

### 3.3 Analysis and testing

The carbon isotope analysis was completed by the State Key Laboratory of Loess and Quaternary Geology at Institute of Earth Environment, Chinese Academy of Sciences. A total of 102 samples were selected and analyzed by the classical phosphoric acid method for carbon isotope analysis. This method requires the first sample pretreatment, that is, CO<sub>2</sub> gas was extracted from the carbonate rock, followed by the use of a MAT252 mass spectrometer to measure the isotopic composition of CO<sub>2</sub> gas which was previously obtained, and the  $\delta^{13}\text{C}$  values of carbonate samples could then be tested. In isotope analysis, the choice of sample is crucial. Fresh, clean, non-polluting samples were selected to avoid carbonate samples that have clearly recrystallized or contain calcite veins. The CO<sub>2</sub> gas was analyzed for carbon isotopes using the MAT252 stable isotope gas mass spectrometer, and the value of  $\delta^{13}\text{C}$  was obtained using Pee Dee belemnite (PDB) standards with an analysis and testing accuracy of 0.1%.

## 4 Test Results and Carbon and Oxygen Isotope Evolution Characteristics

### 4.1 Carbon and oxygen isotope composition characteristics

#### 4.1.1 Carbon isotope composition characteristics

The maximum  $\delta^{13}\text{C}$  of the Permian of the Tongjiang area in Sichuan Province was 4.8‰, the minimum was -0.6‰, and the average was 3.18‰. The  $\delta^{13}\text{C}$  value of the Qixia Formation was between 1.8‰ and 2.7‰, with an average of 2.5‰. The  $\delta^{13}\text{C}$  value of the Maokou Formation was between 2.3‰ and 4.8‰, with an average of 3.6‰. The  $\delta^{13}\text{C}$  value of the Wujiaping Formation was between 0.4‰ and 4.6‰, with an average of 3.0‰. The

**Table 2 Statistical characteristics of carbon isotopic composition of samples from Permian in Tongjiang area, Sichuan province**

$\delta^{13}\text{C}$ value	Qixia Formation	Maokou Formation	Wujiaping Formation	Changxing Formation
Number of samples	5.0	21.0	47.0	27.0
Maximum	2.7	4.8	4.6	4.7
Minimum	1.8	2.3	0.4	-0.6
Average value	2.5	3.6	3.0	3.4

$\delta^{13}\text{C}$  value of the Changxing Formation was between -0.6‰ and 4.7‰, with an average of 3.4‰ (Table 2).

#### 4.1.2 Oxygen isotope composition characteristics

The maximum  $\delta^{18}\text{O}$  of the Permian in the Tongjiang area of Sichuan Province was -3.2‰, the minimum was -10.6‰, and the average was -5.3‰. The  $\delta^{18}\text{O}$  value of the Qixia Formation was between -10.6‰ and -5.3‰, with an average of -8.1‰. The  $\delta^{18}\text{O}$  value of the Maokou Formation was between -8.0‰ and -3.8‰, with an average of -5.6‰. The  $\delta^{18}\text{O}$  value of the Wujiaping Formation was between -7.7‰ and -3.2‰, with an average of -4.9‰. The  $\delta^{18}\text{O}$  value of the Changxing Formation was between -7.0‰ and -4.5‰, with an average of -5.2‰ (Table 3).

### 4.2 Carbon and oxygen isotope evolution characteristics

#### 4.2.1 Carbon isotope evolution characteristics

The  $\delta^{13}\text{C}$  value of the Qixia Formation increased gradually from bottom to top. The  $\delta^{13}\text{C}$  value of middle and lower part of the Maokou Formation was relatively high, and the value of  $\delta^{13}\text{C}$  decreased sharply at the top of the Maokou Formation. The  $\delta^{13}\text{C}$  value of the Wujiaping Formation showed an increasing trend. The  $\delta^{13}\text{C}$  value of the Changxing Formation can be divided into a lower part and an upper part, where the  $\delta^{13}\text{C}$  value of the lower part evolved from high to low, and the value of  $\delta^{13}\text{C}$  decreased to 3.4‰ in the middle and then increased in the upper part. The  $\delta^{13}\text{C}$  value decreased rapidly again at the top of the Changxing Formation at the Permian-Triassic boundary (Fig. 5).

The Permian carbon isotope curve in the Upper Yangtze region showed a high carbon isotope background as a whole. There were three significant negative excursions in the boundary line of the Middle-Late Permian, the Late

**Table 3 Statistical characteristics of oxygen isotopic composition of samples from Permian in Tongjiang area, Sichuan province**

$\delta^{18}\text{O}$ value	Qixia Formation	Maokou Formation	Wujiaping Formation	Changxing Formation
Number of samples	5	21	47	27
Maximum	-5.3	-3.8	-3.2	-4.5
Minimum	-10.6	-8.0	-7.7	-7.0
Average value	-8.1	-5.6	-4.9	-5.2

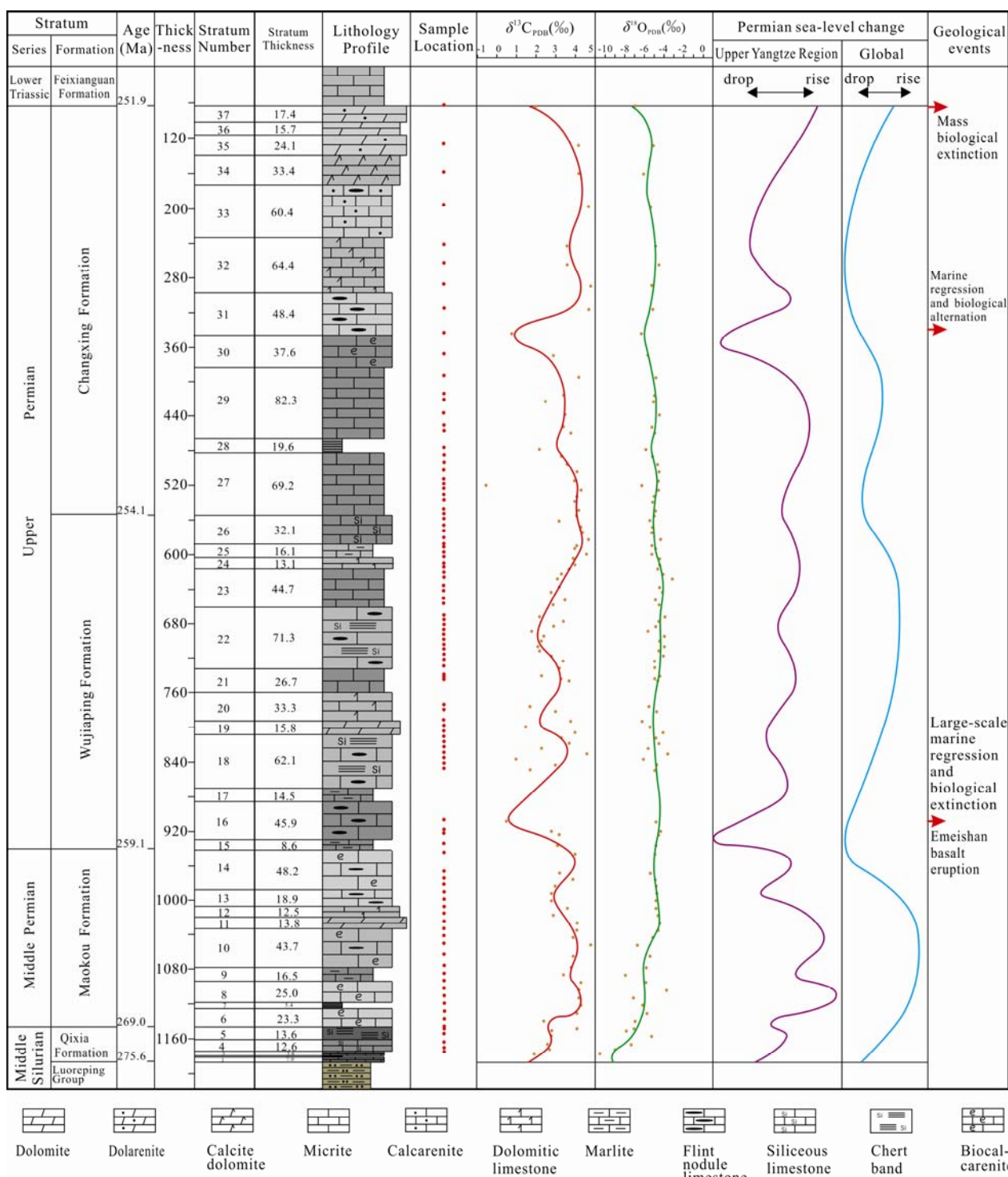


Fig. 5. Permian carbon and oxygen isotope curves and sea-level change curves in Tongjiang, Sichuan Province, China. The sea level change was based on Upper Yangtze data compiled by Chen Zhongqiang, 1995; Qin Jianxiong et al., 1998; Wang Chengshan et al., 1999; and global sea-level change curves from Haq et al., 2008.

Permian, and the end of the Late Permian, and there was a temporary positive balance at the end of the Middle Permian, and the curve abruptly changed at the boundaries of the strata.

#### 4.2.2 Oxygen isotope evolution characteristics

The shape of the Permian oxygen isotope evolution curve of the study area was stable overall. From the Qixia Formation to the top of the Maokou Formation, the oxygen isotope curve gradually presented stable positive

excursions. Thereafter, the oxygen isotope curves of the Wujiaping and Changxing Formations only fluctuated near the positive average value. At the top of the Changxing Formation, which is also the boundary between the Permian and the Triassic, the  $\delta^{18}\text{O}$  value rapidly decreased to  $-7\text{‰}$ , and the oxygen isotope curve showed a significant negative excursion, which was indicative of a decrease in seawater evaporations and salinities, which corresponded to a rapid rise in sea levels.

## 5 Discussions

### 5.1 Discussion of geological significance of carbon and oxygen isotope characteristics

The carbon isotope in geological history is less affected by diagenesis. The  $\delta^{13}\text{C}$  values of the samples can basically represent the carbon isotope compositions in the original formation during a particular period. Therefore, the organic carbon burial rates, sea-level changes, and paleontological evolution during geological history could be recovered by the evolutionary characteristics of the  $\delta^{13}\text{C}$  values (Li Yucheng, 1998; Wang Kun et al., 2016).

#### 5.1.1 Effect of organic carbon burial rates on carbon isotope evolution

The values of  $\delta^{18}\text{O}$  and  $\delta^{13}\text{C}$  in modern seawater are basically maintained at around  $0\text{‰}$  (Chen Jinshi and Chen wenzheng, 1983); Keith et al. (1964) researched 321 carbonate rocks samples of different ages, obtaining an average  $\delta^{13}\text{C}$  value of  $0.56\text{‰}$  (Keith and Weber, 1964); Veizer (1974) suggested that the  $\delta^{13}\text{C}$  value of general marine carbonates ranges from  $-5\text{‰}$  to  $5\text{‰}$  (Veizer, 1974). There was only one negative datum in the  $\delta^{13}\text{C}$  values of the Permian carbonate rocks in the study area, and the rest were positive and ranged from  $0\text{‰}$  to  $5\text{‰}$ , and the  $\delta^{13}\text{C}$  values of 62 of the 100 samples ranged from  $3\text{‰}$  to  $5\text{‰}$ . Therefore, results suggest that there is a strong positive excursion in the  $\delta^{13}\text{C}$  value of marine carbonates during the Permian period in the study area.

The change of  $\delta^{13}\text{C}$  values is closely related to the burial rates of organic carbon during the same period. When there is a large amount of organic carbon quickly buried, it will absorb excess amounts of the light carbon isotope  $^{12}\text{C}$  from the natural carbon pool, which results in the decrease of the light carbon isotope  $^{12}\text{C}$  and a relative increase of isotope  $^{13}\text{C}$  in the carbon pool, which also causes an increase in the heavy carbon isotope  $^{13}\text{C}$  in seawater, which are in equilibrium together, and as a result, a relative rise in carbon isotope  $\delta^{13}\text{C}$  values are induced in marine carbonate rocks that are deposited during the same period, generating positive excursions in the carbon isotope curves. This suggests that the high-speed

accumulation of organic carbon occurred in the Permian period in the study area based on high  $\delta^{13}\text{C}$  values of Permian marine carbonate rocks in the study area.

#### 5.1.2 Effect of sea-level changes on carbon isotope evolution

The carbon isotope curve of Permian carbonate rocks in the study area is similar to the global sea-level change curve (Fig. 5), where abnormal phenomena only occurred at the end of the Permian period, and thus, the carbon isotope curves can generally reflect global sea-level changes. As shown in Figure 5, the carbon isotope evolution curve of the Permian period in the study area is substantially similar to the sea-level change curve during this period. During the Qixia period, due to the warming climate, glaciers melted in the study area, extensive and persistent transgressions occurred in South China, and the  $\delta^{13}\text{C}$  values of the Qixia Formation also continued to rise. During the Maokou period, the sea level continued to rise after the Qixia period, and in the early Maokou period, the sea level rose to the highest point of the Permian, and the  $\delta^{13}\text{C}$  value of the corresponding marine carbonate strata in this period also reached  $4.6\text{‰}$ . Subsequently, the  $\delta^{13}\text{C}$  value decreased with the sea level, and at the end of the Maokou, the largest regression event occurred in the Permian in southern China, the sea level rapidly decreased to the lowest point during the Permian period, the corresponding  $\delta^{13}\text{C}$  value also decreased to  $0.4\text{‰}$ , and the evolution curve of  $\delta^{13}\text{C}$  shows the same fluctuation pattern as the sea-level change curve.

At the initial stage of the Wujiaping period, the sea level began to rise, at this time the  $\delta^{13}\text{C}$  value also increased from  $0.4\text{‰}$ , and in the process of rising, the  $\delta^{13}\text{C}$  value evolution curve and the sea-level change curve had three small-scale fluctuations. In the early part of the Changxing period, the sea level continued to rise accompanied with a  $\delta^{13}\text{C}$  value of  $4.7\text{‰}$ , and subsequently the sea level began to fall, the fluctuation in sea levels also had obvious responses to changes in the  $\delta^{13}\text{C}$  values. However, at the end of the Changxing period, large-scale transgressions occurred in South China,  $\delta^{13}\text{C}$  values did not increase with rising sea levels. By contrast, the  $\delta^{13}\text{C}$  values quickly dropped from  $4.6\text{‰}$  to  $1.9\text{‰}$  at the top of the Changxing Formation. This unusual negative shift was primarily due to the end-Permian mass extinction.

The changes in sea level rise and fall affect the changes in  $\delta^{13}\text{C}$  values, and the evolution of  $\delta^{13}\text{C}$  values are often positively correlated with the rising and falling of sea levels. There are many reasons to consider the negative excursion of carbon isotopes corresponding to the regression. First, when sea level is falling, large quantities of organic matter that were originally in the underwater

environment were exposed to air and then oxidized to  $\text{CO}_2$ , which was enriched with  $^{12}\text{C}$ , and  $\text{CO}_2$  entering the  $\text{CO}_2\text{-HCO}_3^-\text{-CaCO}_3$  system of seawater then resulted in the enrichment of  $^{12}\text{C}$  in seawater. Therefore,  $^{13}\text{C}$  was relatively depleted and the carbon isotope of carbonate moves to negative values. Secondly, during periods of falling sea levels, river transportation was enhanced, and a significant amount of terrestrial organic matter was thus expelled into the ocean by river systems. Since the terrestrial organic matter could not be effectively preserved and oxidized to  $\text{CO}_2$  which is enriched with  $^{12}\text{C}$ , adding it to seawater resulted in the enrichment of  $^{12}\text{C}$  and a reduction of  $^{13}\text{C}$  in seawater, reducing the heavy carbon isotope content in carbonate, and it also caused an increase in the magnitude of changes in heavy carbon isotopes. Thirdly, the decrease in sea level usually corresponded to the development ice age period, in which the surface temperature of seawater decreased, which increased the solubility of  $\text{CO}_2$  and increased the dissolved  $\text{CO}_2$  content in surface seawater, while the corresponding  $^{13}\text{C}$  content decreased, resulting in a decrease in  $\delta^{13}\text{C}$  values of carbonate rocks during this period. Finally, during the period when sea levels fell, the number of marine organisms decreases due to shrinking living space. Thus, the reduction of marine organisms resulted in a decrease in organic matter production, and a large amount of  $^{12}\text{C}$  and  $\text{HCO}_3^-$  cannot be utilized, which resulted in the relative enrichment of  $^{12}\text{C}$  in seawater and decreased carbonate  $\delta^{13}\text{C}$  values and negative excursion of the carbon isotope curve.

The positive excursion of the carbon isotope curve corresponded to a rise in sea level, which caused marine organisms to flourish and biological effects to increase, whereby the metabolism of the organisms and the photosynthesis of the algae continuously consumed the  $^{12}\text{C}$  in the seawater, and the production of organic matter increased. Living space can increase in periods of rising sea levels, and the possibility of oxidation of organic substances is reduced, thus quickly and efficiently preserving it. If evaporation is involved in this process and a considerable part of the  $^{12}\text{C}$  preferentially escapes in the gas phase, these processes both result in a decrease in the light carbon isotopes in seawater, and a relative enrichment by heavy carbon isotopes, resulting in an increase in the carbon isotope values of carbonate and a positive excursion in the carbon isotope curve. In addition, sea-level rise results in a weakening of fluviation, resulting in the recession and reduction of the oxidation area associated with land previously exposed to air. Erosion products are also reduced and the amount of organic carbon expelled into the ocean from river systems is also reduced. As the impact of terrestrial organic matter

decreases, it results in a relative lack of  $^{12}\text{C}$  and enrichment of  $^{13}\text{C}$  in seawater. The  $\delta^{13}\text{C}$  value of the balanced carbonate correspondingly increases, and there is a carbon isotope curve positive excursion.

### 5.1.3 Influence of prospering or declining biology on carbon isotope evolution

There are dioxide carbon pool and reduction carbon pool of two major carbon pools in nature, the excursion of  $\delta^{13}\text{C}$  values are caused by a relative change in the ratio between the two major carbon pools (Mackenzie and Pigott, 1981). The oxide carbon pool is mainly carbonate sediments with relatively high  $\delta^{13}\text{C}$  values (modern value is 0.4‰) (Arthur et al., 1985), while a reduction in the carbon pool is organic carbon or biosphere carbon pools with relatively low  $\delta^{13}\text{C}$  values (average is -25‰), because of the biological fractionation (Arthur et al., 1985), the difference  $\delta^{13}\text{C}$  values between the two major carbon pools is approximately 25‰. When the carbon in the biosphere carbon pool changes, the quantity of carbon in the carbonate carbon pool will inevitably change, and the values of  $\delta^{13}\text{C}$  will change accordingly.

During the Permian in the study area, there were three large mass extinctions of biological organisms. The first occurred from the end of the Maokou period to the initial stage of the Wujiaping period, when sea levels fell, and a large number of foraminifera, ammonites, brachiopods, and corals went extinct in varying degrees. As shown in Figure 5, the evolution curve of  $\delta^{13}\text{C}$  shows a significant negative excursion from the end of the Maokou period to the initial stage of the Wujiaping period, and the  $\delta^{13}\text{C}$  values was reduced to 0.4‰. The second mass extinction occurred between the Wujiaping and Changxing periods (He Xilin and Shen Shuzhong, 1988), when a large-scale organism alteration occurred, as Figure 5 also clearly shows. After the Wujiaping period, there was a gradual negative excursion of the  $\delta^{13}\text{C}$  value, which indicated that old species at this time were greatly reduced and many disappeared. The  $\delta^{13}\text{C}$  values in the middle of the Changxing Formation was reduced to a minimum and after the middle of the Changxing period to the Late Permian,  $\delta^{13}\text{C}$  values began to rise in a positive excursion, indicating that there was a recovery of new species after the old species declined the study area. The third extinction occurred at the end of the Changxing period, which corresponds to the Permian-Triassic boundary. The largest mass extinction in history occurred in this period (Wignall and Twitchett, 1996). At the end of the Changxing period, as shown in Figure 5, at the boundary between the Permian and Triassic, the carbon isotope curve rapidly shifted to a negative excursion with the  $\delta^{13}\text{C}$  values reduced sharply from 4.1‰ to 1.9‰.

The changes in  $\delta^{13}\text{C}$  values of the Permian in the study area were closely related to the rise and fall of biological organisms, with the prosperity of these organisms corresponding to the high values of carbon isotopes, while the mass extinction period corresponded to the low values of carbon isotopes. In periods of biological prosperity, the increasing marine biological activity and burial of organic carbon can increase consumption of  $^{12}\text{C}$  in the atmosphere, while it reduces the  $^{12}\text{C}$  reduction, causing a decrease in the  $^{12}\text{C}$  exchange from seawater to the atmosphere, which finally results in a relative increase in seawater  $^{13}\text{C}$ , so that the values of  $\delta^{13}\text{C}$  in carbonate rocks increased and the carbon isotope curve shifts with positive excursion.

When the old species of organisms were subject to mass extinction, the new species did not recover during this gap, marine biological activity weakened, the burial of organic carbon decreased, the number of  $^{12}\text{C}$  in organic carbon pool drastically decreased, and a large amount of the  $^{12}\text{C}$  was transferred from the atmosphere to the seawater due to the circulation of the atmosphere and seawater. This resulted in a decrease of  $\delta^{13}\text{C}$  in carbonate rocks deposited during the same period, and led to the negative excursion of the carbon isotope curves.

#### 5.1.4 Effect of volcanic activity on carbon isotope evolution

The composition of marine organic carbon isotopes was directly affected by the  $^{12}\text{C}/^{13}\text{C}$  ratio of dissolved carbon in seawater and the total amount of  $\text{CO}_2$ . The most direct effect of volcanism was associated with its huge amounts of  $\text{CO}_2$  rich in  $^{12}\text{C}$  (Korte et al., 2010; Self et al., 2014; Bond et al., 2015), so that the concentration of dissolved  $^{12}\text{C}$  during the same period of atmosphere and seawater increased, leading to a steep drop in  $\delta^{13}\text{C}_{\text{org}}$  in a short period of volcanic activity (Self et al., 2006; Yang Zhengyu et al., 2009; Hu Qing et al., 2011; Wei Hengye et al., 2012). In addition, a large amount of  $\text{CO}_2$  released by large-scale volcanic eruptions causes a rise in surface temperature, which led to a reduction of the carbon isotope fractionation coefficient in seawater. As a result the  $^{13}\text{C}$  value of the sedimentary marine carbonate also decreased (Peng Bingxia et al., 2006). In addition, volcanic eruptions, tectonic uplifts and fractures caused by mantle plume activity caused the submerged gas hydrates to rapidly release a large amount of  $\text{CH}_4$  (methane) and  $\text{CO}_2$ . Methane released into the ocean can react with oxygen and produce a large amount of  $\text{CO}_2$ , which likely caused significant changes in the oceanic-atmosphere carbon transformation system, including a decrease of the carbon isotope composition, global warming, and mass extinction (Heydari et al., 2008).

#### 5.1.5 Significance of oxygen isotopes

$\delta^{18}\text{O}$  values of original sedimentary carbonate rocks would strongly change after diagenesis because of the isotopic exchange and thermal decomposition of carbonate rocks (Li Zhongxiong and Guan Shiping, 2001; Guo Fusheng et al., 2003). Although it is difficult to use the values of  $\delta^{18}\text{O}$  measured today to quantitatively reflect the original sedimentary characteristics of a certain period, the value of  $\delta^{18}\text{O}$  can reflect changes in seawater temperatures and salinity values to a certain extent (Mattews and Poore, 1980; Hoffman et al., 1991; Yan Zhaobin et al., 2005). The primary reasons for oxygen isotope fractionation are associated with the evaporation of seawater and the addition of fresh water, so  $\delta^{18}\text{O}$  is affected by the superposition of various factors such as sea-level changes, temperature changes, salinity changes, and deep ocean water (Li Rongxi et al., 2007) characteristics.  $\delta^{18}\text{O}$  is mostly affected by the temperature and concentration of the medium, and when some of the carbonate rocks formed, the oxygen isotope composition was largely dependent on the temperature. A temperature decrease is accompanied by a rise in  $\delta^{18}\text{O}$ , and a temperature increase is accompanied by a decrease in the  $\delta^{18}\text{O}$  value (Li Xin et al., 2009). Evaporation of seawaters also leads to an increase in seawater salinity, which promotes the fractionation of oxygen isotopes. Therefore, the greater the salinity, the higher value of  $\delta^{18}\text{O}$  in seawater, whereas lower salinity values are associated with lower values of  $\delta^{18}\text{O}$  in seawaters.

At the top of the Changxing Formation, which is also boundary between the Permian and the Triassic, the  $\delta^{18}\text{O}$  value rapidly decreased to  $-7\text{‰}$ , and the oxygen isotope curve displayed a significant negative excursion, indicating a decrease in seawater evaporation and salinities, which corresponded to the rapid sea-level rise.

#### 5.2 The geological significance of the three negative excursions of carbon isotope

The first negative excursion of the carbon isotope curve at the boundary of the Middle and Late Permian reflects the Emeishan flood basalt eruptions, sea-level regression events, and mass extinction events in the Upper Yangtze region. The negative excursion of  $\delta^{13}\text{C}$  dropped to its lowest value at the boundary of the Middle and Late Permian. Although the Emeishan Basalt eruptions occurred at this time (He Bin et al., 2005; Peng Bingxia et al., 2006; Xu Yigang et al., 2007; Sun et al., 2010; Zhong et al., 2014; Xu Yigang et al., 2017), the largest marine regression of the Permian occurred in South China, and sea levels fell, which corresponded to changes in the global sea level (Chen et al., 2009; Xue et al., 2015). In addition, the decrease in the global large-scale sea level at

the end of the Guadaloupean led to the absence of a wide range of GLB formations that brought uncertainties of biodiversity (Haq et al., 2008), and a large number of foraminifera, ammonite, brachiopods, and coral species went extinct to varying degrees (Zhang Liqin., 2013; Wang, 2013; Kofukuda et al., 2014; Bond et al., 2015; Arefifard, 2018).

The second negative excursion of the carbon isotope curve in the Late Permian reflects marine regression and biological replacement events. The negative excursion of the carbon isotopes in the Late Permian indicated the sea level declined, which corresponded to the relative sea-level changes in the Upper Yangtze region, while it also indicated a large-scale biological replacement during that period. The number of old genera and species decreased and disappeared (such as brachiopods, fusulinids and foraminifera) (Kofukuda et al., 2014; Arefifard, 2018). The decrease and extinction of organisms resulted in a reduction of heavy carbon isotopes and a decrease of the  $\delta^{13}\text{C}$  values in seawater.

The third negative excursion of the carbon isotope curve at the end-Permian reflects the largest mass extinction in history. The negative excursion of the carbon isotope curve at the end-Permian did not correspond with a decline in sea level. On the contrary, large-scale transgression and sea level rise occurred in South China during this period (Haq et al., 2008). The reason for this unusual negative excursion was the largest biological extinction event in history, more than 90% of marine species and 70% of terrestrial organisms went extinct (such as brachiopods, corals, fusulinids, foraminifera, ostracods, cephalopods, etc.), and the ultimate extinction rate reached 94% (Peng et al., 2007; Yin Hongfu and Song Haijun, 2013; Erwin, 2015).

## 6 Conclusions

(1) The Permian carbon isotope curve in the northern part of the Upper Yangtze region showed relatively high background carbon isotope baseline concentrations with three negative significant excursions. The three negative significant excursions were identified at the Middle–Late Permian boundary, the Late Permian, and the end-Permian.

(2) The three distinct negative excursions of carbon isotopes are good indicators of the Permian global biological mass extinction events and the eruption of the Emeishan flood basalts in the Upper Yangtze region. The first negative excursion of the carbon isotope at the boundary line of the Middle–Late Permian reflects the eruption of the Emeishan flood basalts, decreasing sea levels, and different biological extinction events in varying

degrees. The second negative excursion of the carbon isotope at the late period of Late Permian images sea level decreasing and large-scale biological replacement events; The third negative excursion of the carbon isotope at the last stage of Late Permian, which unusually corresponds to sea-level rising rather than sea level decreasing, reveals the biological mass extinction events at the end-Permian. The first negative excursion at the Middle–Late Permian boundary reflected the eruption of the Emeishan flood basalts, a decrease in sea level, and biological extinction events of different genera in varying degrees. The second negative excursion in the late Late Permian included decreasing sea level and large-scale biological replacement events. The third negative excursion of the carbon isotope at the end of the Permian unusually corresponded to a rise rather than a decrease in sea level, and it revealed a biological mass extinction event at the end of the Permian.

## Acknowledgments

This research was financially supported by The National Key Research Project of China (No.2016YFC0601003), Northwest University Graduate Innovation and Creativity Funds (YZZ17198) and the National Natural Science Foundation of China (Grants No. 41390451 and No. 41172101). We thank the anonymous reviewer and the Editor for their comments and suggestions, which significantly improved the quality of the manuscript, and we would also thank Prof. Yunpeng Dong and Prof. Jian Xu from Northwest University, China for their insightful discussions and suggestions.

Manuscript received Dec. 15, 2017

accepted Jul. 27, 2018

edited by Liu Lian

## References

- Arefifard, S., 2018. Sea level drop Palaeoenvironmental change and related Biotic Responses across Guadalupian-Lopingian boundary in Southwest, North and Central Iran. *Geological Magazine*, 155(4): 921–943.
- Arthur, M.A., Dean, W.E., and Schlanger, S.O., 1985. Variations in the global carbon cycle during the Cretaceous related to climate, volcanism, and changes in atmospheric CO<sub>2</sub>. *Carbon Cycle & Atmospheric Co Natural Variations Archean to Present*, 32: 504–529.
- Bond, D.P.G., Wignall, P.B., Joachimski, M.M., Sun, Y.D., Savov, I., Grasby, S.E., Beauchamp, B., and Blomeier, D.P.G., 2015. An abrupt extinction in the Middle Permian (Capitanian) of the Boreal Realm (Spitsbergen) and its link to anoxia and acidification. *Geological Society of America Bulletin*, 127(9): 1411–1421.
- Burgess, S.D., Bowring, S., and Shen, S.Z., 2014. High-

- Precision timeline for earth's most severe extinction. *Proceedings of the National Academy of Sciences of the United States of America*, 111(9): 3316–3321.
- Cao Changqun, WangWei and JinYugan, 2002. Carbon isotope excursions across the Permian–Triassic boundary in the Meishan section, Zhejiang Province, China. *Chinese Science Bulletin (English Edition)*, 47(13):1125–1129.
- Chen Jinshi and Chen Wenzheng, 1983. *Introduction of Geology of Carbon Isotope*. Beijing: Geological Publishing House (in Chinese).
- Chen Zhongqiang, 1995. The Late Permian global flooding events. *Sedimentary Facies and Palaeogeography*, 15(3): 34–39 (in Chinese with English abstract).
- Chen, B., Joachimski, M.M., Shen, S.Z., Lambert, L.L., Lai, X.L., Wang, X.D., Chen, J., and Yuan, D.X., 2013. Permian ice volume and palaeoclimate history: oxygen isotope proxies revisited. *Gondwana Research*, 24(1): 77–89.
- Chen, Z.Q., George, A.D., and Yang, W.R., 2009. Effects of Middle–Late Permian sea–level changes and mass extinction on the Formation of the Tieqiao Skeletal Mound in the Laibin Area, South China. *Australian Journal of Earth Sciences*, 56 (6): 745–763.
- Coogan, L.A., and Dosso, S.E., 2015. Alteration of ocean crust provides a strong temperature dependent feedback on the geological carbon cycle and is a primary driver of the Sr–isotopic composition of seawater. *Earth & Planetary Science Letters*, 415: 38–46.
- Cui, Y., Bercovici, A., Yu, J.X., Kump, L.R., Freeman, K.H., Su, S.G., and Vajda, V., 2017. Carbon cycle perturbation expressed in terrestrial Permian–Triassic boundary sections in South China. *Global & Planetary Change*, 148: 272–285.
- Deng Hongying and Shou Jianfeng, 1999. Characteristics of Permian depositional sequences in South China. *Marine Origin Petroleum Geology*, 4(2): 9–15 (in Chinese).
- Dong, Y.P., and Santosh, M., 2016. Tectonic architecture and multipletrogeny of the Qinling Orogenic Belt, Central China. *Gondwana Research*, 29(1): 1–40.
- Dong, Y.P., Zhang, X.N., Liu, X.M., Li, W., Chen, Q., Zhang, G.W., Zhang, H.F., Yang, Z., Sun, S.S., and Zhang, F.F., 2015. Propagation tectonics and multiple accretionary processes of the Qinling Orogen. *Journal of Asian Earth Sciences*, 104: 84–98.
- Du Xiaodi, Liu Wanzhu and Wang Dongpo, 1994. Carbon and oxygen isotope and sea–level changes: the Upper Sinian–Ordovician carbon and oxygen isotopic section in Xinjiang Keping Area as an Example. *Global Geology*, 13(3): 120–123 (in Chinese).
- Erwin, D.H., 2015. Extinction: how life on earth nearly ended 250 million years ago. *Biologist*, 311(5769): 1868–1869.
- Goddéris, Y., Hir, G.L., Macquain, M., Donnadieu, Y., Hubert–Théou, L., Dera, G., Aretz, M., Fluteau, F., Li, Z.X., and Halverson, G.P., 2017. Paleogeographic forcing of the strontium isotopic cycle in the Neoproterozoic. *Gondwana Research*, 42: 151–162.
- Guo Fusheng, Peng Huaming, Pan Jiayong, Du Yangsong, Liu Linqing, Luo Nenghui, Rao, Minghui and Wang Zhengqi, 2003. A probe into the carbon and oxygen isotopic characteristics of the Cambrian carbonate rocks in Jiangshan, Zhejiang and its paleo–environment significance. *Journal of Stratigraphy*, 27(4): 289–297 (in Chinese with English abstract).
- Guo Qingjun, Liu Congqiang, Harald Strauss, Tatiana Goldberg, Zhu Maoyan, Pi Daohui and Wang Jian, 2006. Organic carbon isotope geochemistry of the neoproterozoic Doushantuo Formation, South China. *Acta Geologica Sinica (English Edition)*, 80(5): 670–683.
- Haq, B.U., and Schutter, S.R., 2008. A chronology of Paleozoic sea–level changes. *Science*, 322(5898): 64–68.
- He Bin, XuYigang, Wang Yamei and Xiao Long, 2005. Nature of the Dongwu movement and its temporal and spatial evolution. *Earth science*, 30(1): 89–96 (in Chinese with English abstract).
- He Xilin and Shen Shuzhong, 1988. Study on biological alteration near the Permian and Triassic boundary in Zhongliangshan Area, Chongqing. *Journal of Stratigraphy*, 12 (4): 268–272 (in Chinese).
- He, B., Xu, Y.G., Huang, X.L., Luo, Z.Y., Shi, Y.R., Yang, Q.J., and Yu, S.Y., 2007. Age and duration of the Emeishan flood volcanism, SW China: Geochemistry and SRIMP zircon U–Pb dating of silicic ignimbrites, post–volcanic Xuanwei Formation and clay tuff at the Chaotian section. *Earth & Planetary Science Letters*, 255(3): 306–323.
- Hermann, E., Hochuli, P.A., Bucher, H., Brühwiler, T., Hautmann, M., Ware, D., and Roohi, G., 2011. Terrestrial ecosystems on North Gondwana following the end–Permian mass extinction. *Gondwana Research*, 20(2): 630–637.
- Heydari, E., Arzani, N., and Hassanzadeh, J., 2008. Mantle plume: the invisible serial killer–application to the Permian–Triassic boundary mass extinction. *Palaeogeography, Palaeoclimatology, Palaeoecology*, 264(1–2): 147–162.
- Hoffman, A., Gruszczynski, M., and Malkowski, K., 1991. On the interrelationship between temporal trends in  $\delta^{13}\text{C}$ ,  $\delta^{18}\text{O}$ , and  $\delta^{34}\text{Sr}$  in the world ocean. *The Journal of Geology*, 99(3): 355–370.
- Hu Qing, Cao Jun, Huang Junhua, Yu Jianxin, Zhang Ning and Feng Qinglai, 2011. Variation of organic carbon isotope and Bio–geochemical significances across the Permian–Triassic boundary at Xinmin section, Guizhou, South China. *Geological review*, 57(3): 305–315 (in Chinese with English abstract).
- Huang Sijing, Huang Keke, Lv Jie and Lan Yefang, 2012. Carbon isotopic composition of early Triassic marine carbonates, eastern Sichuan Basin. *Scientia Sinica (Terrae)*, 42 (10): 1508–1522.
- Huang Sijing, Qing Hairuo, Huang Peipei, Hu Zuowei, Wang Qingdong, Zou Mingliang and Liu Haonian, 2008. Evolution of strontium isotopic composition of seawater from Late Permian to Early Triassic based on study of marine carbonates, Zhongliang Mountain, Chongqing. *Science in China (Series. D)*, 51(4): 528–539.
- Huang Sijing, Shi He, Zhang Meng, Shen Licheng, Liu Jie and Wu Wenhui, 2001. Strontium isotope evolution and global sea–level changes of Carboniferous and Permian marine carbonate, Upper Yangtze Platform. *Acta Sedimentologica Sinica*. 19(4):481–487 (in Chinese with English abstract).
- Huang Sijing, Wu Sujuan, Sun Zhilei, Pei Changrong and Hu Zuowei, 2005. Seawater strontium isotopes and paleo–oceanic events over the past 260Ma. *Earth Science Frontiers*. 12(2): 133–141 (in Chinese with English abstract).
- Isbell, J.L., Miller, M.F., Wolfe, K.L., and Lenaker, P.A., 2003. Timing of Late Paleozoic glaciation in Gondwana: was glaciation responsible for the development of northern

- hemisphere cyclothem? *Geological Society of America Special Papers*, 370: 5–24.
- Isozaki, Y., 2009. Illawarra reversal: the fingerprint of a superplume that triggered Pangean breakup and the end-Guadalupian (Permian) mass extinction. *Gondwana Research*, 15(3): 421–432.
- Isozaki, Y., Kawahata, H., and Minoshima, K., 2007b. The Capitanian (Permian) Kamura cooling event: the beginning of the Paleozoic–Mesozoic transition. *Palaeoworld*, 16(1–3): 16–30.
- Isozaki, Y., Shimizu, N., Yao, J., Ji, Z., and Matsuda, T., 2007a. End-Permian extinction and volcanism-induced environmental stress: The Permian–Triassic boundary interval of lower-slope facies at Chaotian, South China. *Palaeogeography, Palaeoclimatology, Palaeoecology*, 252(1–2): 218–238.
- Jin Yugan, Wang Xiangdong, Shang Qinghua, Wang Yue and Sheng Jinzhang, 1999. Chronostratigraphic subdivision and correlation of the Permian in China. *Acta Geologica Sinica*, 73(2): 97–108 (in Chinese with English abstract).
- Keith, M.L., and Weber, J.N., 1964. Carbon and oxygen isotopic composition of selected limestones and fossils. *Geochimica et Cosmochimica Acta*, 28(10–11): 1787–1816.
- Kofukuda, D., Isozaki, Y., and Igo, H., 2014. A remarkable sea-level drop and relevant biotic responses across the Guadalupian–Lopingian (Permian) boundary in low-latitude Mid-Panthalassa: irreversible changes recorded in accreted Paleo-Aatollimestones in Akasaka and Ishiyama, Japan. *Journal of Asian Earth Sciences*, 82(3): 47–65.
- Korte, C., Jasper, T., Kozur, H.W., and Veizer, J., 2006.  $^{87}\text{Sr}/^{86}\text{Sr}$  record of Permian seawater. *Palaeogeography, Palaeoclimatology, Palaeoecology*, 240(1–2): 89–107.
- Korte, C., Pande, P., Kalia, P., Kozur, H.W., Joachimski, M.M., and Oberhänsli, H., 2010. Massive volcanism at the Permian–Triassic boundary and its impact on the isotopic composition of the ocean and atmosphere. *Journal of Asian Earth Sciences*, 37(4): 293–311.
- Lan Yefang, Huang Sijing, Ma Yongkun, Zhou Xiaokang and Wei Zhe, 2016. Genesis of negative carbon and oxygen isotopic composition of carbonate rocks in Lower Miocene Zhujiang Formation, Pearl river mouth Basin. *Geological review*, 62(4): 915–928 (in Chinese with English abstract).
- Li Guohui, Li Xiang, Song Shujun, Song Wenhui and Yang Xinan, 2005. Dividing Permian into 3 series and its significance in Sichuan Basin. *Natural Gas Exploration and Development*, 28(3): 20–25 (in Chinese with English abstract).
- Li Renwei, Lu Jialan, Zhang Shukun and Lei Jiabin, 1999. Organic carbon isotopes of the Sinian and Early Cambrian black shales on Yangtze Platform, China. *Science in China (Series. D)*, 42(6): 595–603.
- Li Rongxi, Wei Jiayong, Xiao Jiafei, Wang Xingli and Lehrmann D.J., 2007. Response of carbon and oxygen isotopic geochemistry to transgressive systems tract: an example from Triassic stratigraphy in southwestern Guizhou Province. *Journal of Earth Science and Environment*, 29(1): 1–5 (in Chinese with English abstract).
- Li Xia, Hu Mingyi and Li Shixiang, 2005. Carbonate gentle slope deposition of Permian in Longmen Mountain–MiCangshan front. *Journal of Oil and Gas Technology*, 27(1): 36–37 (in Chinese).
- Li Xin, LuoShunshu, Kuang Hongwei, Su Jie and Yin Xiao, 2009. Carbon and oxygen isotopic evolution in the carbonate rocks from the Wumishan Formation in Lingyuan, western Liaoning. *Sedimentary Geology and Tethyan Geology*, 29(2): 107–111 (in Chinese with English abstract).
- Li Yucheng, 1998. The carbon isotope cyclostratigraphic response to sea level change in Upper Permian limestones from South China. *Acta Sedimentologica Sinica*, 16(3): 52–57 (in Chinese).
- Li Zhongxiong and Guan Shiping, 2001. Sedimentary cycle and strontium, carbon, oxygen isotopes of the Silurian at Luguhu region in Ninglang county of western margin of Yangtze platform. *Journal of Palaeogeography*, 3(4): 69–76 (in Chinese with English abstract).
- Liu Shuhua, Huang Jiayi, Chen Lin, Yang Liang, Chen Qiong, Mi Xiaojian, He Haibo, Deng Xiaomin, Peng Xiaotao, Li Hanjie and Zhou Houyun, 2016. A speleothem  $\delta^{13}\text{C}$  record and control mechanism during 120–130ka B. P. from NE Sichuan, Central China. *Acta Geologica Sinica*, 90(2): 334–340 (in Chinese with English abstract).
- Liu, X.C., Wang, W., Shen, S.Z., Gorgij, M.N., Ye, F.C., Zhang, Y.C., Furuyama, S., Kano, A., and Chen, X.Z., 2013. Late Guadalupian to Lopingian (Permian) carbon and strontium isotopic chemostratigraphy in the Abadeh section, central Iran. *Gondwana Research*, 24(1): 222–232.
- Luo Zhenyu, Xu Yigang, He Bin, Shi Yuruo and Huang Xiaolong, 2007. Geochronologic and petrochemical evidence for the genetic link between the Maomaogou nepheline syenites and the Emeishan large igneous province. *Chinese Science Bulletin*, 52(7): 949–958.
- Mackenzie, F.T., and Pigott, J.D., 1981. Tectonic controls of Phanerozoic sedimentary rock cycling. *Journal of the Geological Society*, 138(2): 183–196.
- Magaritz, M., Bart, R., Baud, A., and Holser, W., 1988. The carbon–isotope shift at the Permian/Triassic boundary in the Southern Alps is Gradual. *Nature*, 331(6154): 337–339.
- Mattews, R.K., and Poore, R.Z., 1980. Tertiary  $\delta^{18}\text{O}$  record and glacio–eustatic sea–level fluctuations. *Geology*, 8(10): 501–504.
- Michael, J.M., and Chris, H., 2006. Carbon isotope Chemostratigraphy of the Llandovery in Arctic Canada: implications for global correlation and sea–level change. *GFF*, 128(2): 173–180.
- Munnecke, A., Calner, M., Harper, D.A.T., and Servaisad, T., 2010. Ordovician and Silurian sea–water chemistry, sea level, and climate: a synopsis. *Palaeogeography, Palaeoclimatology, Palaeoecology*, 296(3): 389–413.
- Payne, J.L., Lehrmann, D.J., Wei, J.Y., Orchard, M.J., Schrag, D.P., and Knoll, A.H., 2004. Large perturbations of the carbon cycle during recovery from the End–Permian extinction. *Science*, 305(5683): 506–509.
- Payne, J.L., Meyer, K.M., Yu, M., Jost, A.B., and Kelley, B.M., 2011.  $\delta^{13}\text{C}$  evidence that high primary productivity delayed recovery from End–Permian mass extinction. *Earth & Planetary Science Letters*, 302(3): 378–384.
- Peng Bingxia, Wang Yuejun, Fan Weiming and Peng Touping, 2006. Carbon isotope composition changes of Maokouian–Wuchiapingian and the environmental effect of Emeishan large igneous province at Lekang section, Guizhou province. *Geochimica*, 35(2): 126–132 (in Chinese with English abstract).
- Peng, Y.Q., Shi, G.R., Gao, Y.Q., He, W.H., and Shen, S.Z.,

2007. How and why did the Lingulidae (Brachiopoda) not only survive the End-Permian mass extinction but also thrive in its Aftermath? *Palaeogeography, Palaeoclimatology, Palaeoecology*, 252(1–2): 118–131.
- Qian Xin, Feng Qinglai, Wang Yuejun and Zhang Zhibin, 2016. Geochemical and Geochronological constraints on the origin of the Meta-basic volcanic rocks in the Tengtaohe Zone, Southeast Yunnan. *Acta Geologica Sinica* (English Edition), 90(2): 669–683.
- Qin Jianxiong, Chen Hongde and Tian Jingchun, 1998. The global sea-level changes during the Permian. *Sedimentary facies and palaeogeography*, 18(6): 40–47 (in Chinese with English abstract).
- Qiu, Z., Wang, Q.C., Zou, C.N., Yan, D.T., and Wei, H.Y., 2014. Transgressive-regressive sequences on the slope of an isolated carbonate platform (Middle-Late Permian, Laibin, South China). *Facies*, 60(1): 327–345.
- Railsback, L.B., Ackerly, S.C., Anderson, T.F., and Cisne, J.L., 1990. Paleontologic and isotopic evidence for warm saline deep waters in Middle Ordovician oceans. *Nature*, 343(6254): 156–159.
- Sanson-Barrera, A., Hochuli, P.A., Bucher, H., Schneebeli-Hermann, E., Weissert, H., Adatte, T., and Bernasconi, S.M., 2015. Late Permian–Earliest Triassic high-resolution organic carbon isotope and palynofacies records from KapStosch (East Greenland). *Global and Planetary Change*, 133: 149–166.
- Self, S., Schmidt, A., and Mather, T.A., 2014. Emplacement characteristics, time scales, and volcanic gas release rates of continental flood basalt eruptions on Earth. *Geological Society of America Special Papers*, 505: 319–337.
- Self, S., Widdowson, M., Thordarson, T., and Jay, A.E., 2006. Volatile fluxes during flood basalt eruptions and potential effects on the global environment: a decade perspective. *Earth & Planetary Science Letters*, 248: 518–532.
- Shellnutt, J.G., Bhat, G.M., Wang, K.L., Brookfield, M.E., Jahn, B.M., and Dostal, J., 2014. Petrogenesis of the flood basalts from the Early Permian Panjal Traps, Kashmir, India: Geochemical evidence for shallow melting of the mantle. *Lithos*, 204(3): 159–171.
- Shen Shuzhong, Zhu Maoyan, Wang Xiangdong, Li Guoxiang, Cao Changqun and Zhang Hua, 2010. A comparison of the biological, geological events and environmental backgrounds between the Neoproterozoic–Cambrian and Permian–Triassic transitions. *Science China: Earth Sciences*, 53(12): 1873–1884.
- Shen, S.Z., Crowley, J.L., Wang, Y., Bowring, S.A., Erwin, D.H., Sadler, P.M., Cao, C.Q., Rothman, D.H., Henderson, C.M., Ramezani, J., Zhang, H., Shen, A., Wang, X.D., Wang, W., Mu, L., Li, W.Z., Tang, Y.G., Liu, X.L., Liu, L.J., Zeng, Y., Jiang, Y.F., and Jin, Y.G., 2011. Calibrating the End-Permian mass extinction. *Science*, 334(6061): 1367–1372.
- Song, H.J., Wignall, P.B., Tong, J.N., Song, H.Y., Chen, J., Chu, D.L., Tian, L., Luo, M., Zong, K.Q., Chen, Y.L., Lai, X.L., Zhang, K.X., and Wang, H.M., 2015. Integrated Sr isotope variations and global environmental changes through the Late Permian to Early Triassic. *Earth & Planetary Science Letters*, 424: 140–147.
- Sun, Y.D., Lai, X.L., Wignall, P.B., Widdowson, M., Alie, J.R., Jiang, H.S., Wang, W., Yan, C.B., Bond, D.P.G., and Védrine, S., 2010. Dating the onset and nature of the Middle Permian Emeishan large igneous province eruptions in SW China using conodont biostratigraphy and its bearing on Mantle Plume Uplift Models. *Lithos*, 119(1–2): 20–33.
- Van der Meer, D.G., Van den Berg van Saparoea, A.P.H., Van Hinsbergen, D.J.J., Van de Weg, R.M.B., Godderis, Y., Le Hir, G., and Donnadieu, Y., 2017. Reconstructing first-order changes in sea level during the Phanerozoic and Neoproterozoic using strontium isotopes. *Gondwana Research*, 44: 22–34.
- Veevers, J.J., and Powell, C.M., 1987. Late Paleozoic glacial episodes in Gondwana land reflected in transgressive-regressive depositional sequences in Euramerica. *Geological Society of America Bulletin*, 98(4): 475–487.
- Veizer, R.D.J., 1974. Strontium as a tool in facies analysis. *Journal of Sedimentary Research*, 44(1): 93–115.
- Wang Chengshan, Li Xianghui, Chen Hongde and Qin Jianxiong, 1999. Permian sea-level changes and rising-falling events in South China. *Acta Sedimentologica Sinica*, 17(4): 536–541 (in Chinese with English abstract).
- Wang Qingchen and Cai Ligu, 2007. Phanerozoic tectonic evolution of South China. *Acta Geologica Sinica*, 81(8): 1025–1040 (in Chinese with English abstract).
- Wang, X.D., and Sugiyama, T., 2000. Diversity and extinction patterns of Permian coral faunas of China. *Lethaia*, 33(4): 285–294.
- Wang, X.D., Qie, W.K., Sheng, Q.Y., and Ueno, K., 2013. The Carboniferous and Lower Permian of South China, sedimentologic cycles and biotic events. *Special Publications of Journal of Geological Society of London*, 376(1): 33–46.
- Wang, X.D., Shen, S.Z., and Somerville, I.D., 2009. Carboniferous and Permian biota, integrative stratigraphy, sedimentology, palaeogeography, and palaeoclimatology—an introduction. *Palaeoworld*, 18(2): 77–79.
- Wang Kun, Hu Suyun, Li Wei, Liu Wei, Huang Qingyu, Ma Kui and Shi Shuyuan, 2016. Depositional System of the Carboniferous Huanglong Formation, Eastern Sichuan Basin: Constraints from Sedimentology and Geochemistry. *Acta Geologica Sinica* (English Edition), 90(5): 1795–1808.
- Wei Hengye, Chen Daizhao, Yu Hao and Wang Jianguo, 2012. End-Guadalupian mass extinction and negative carbon isotope excursion at Xiaojiaba, Guangyuan, Sichuan. *Science China: Earth Sciences*, 55(9): 1480–1488.
- Wei, H.Y., Yu, H., Wang, J.G., Qiu, Z., Xiang, L., and Shi, G., 2015. Carbon isotopic shift and its cause at the Wuchiapingian–Changhsingian boundary in the Upper Permian at the Zhaojiaba Section, South China: evidences from multiple geochemical proxies. *Journal of Asian Earth Sciences*, 105(6): 270–285.
- Wenzel, B., and Joachimski, M.M., 1996. Carbon and oxygen isotopic composition of Silurian Brachiopods (Gotland/Sweden): Palaeoceanographic implications. *Palaeogeography, Palaeoclimatology, Palaeoecology*, 122(1–4): 143–166.
- Wignall, P.B., and Twitchett, R.J., 1996. Oceanic anoxia and the end Permian mass extinction. *Science*, 272(5265): 1155–1158.
- Wignall, P.B., Sun, Y., Bond, D.P.G., Izon, G., Newton, R.J., Védrine, S., Widdowson, M., Ali, J.R., Lai, X.L., Jiang, H.S., Cope, H., and Bottrell, S.H., 2009. Volcanism, mass extinction, and carbon isotope fluctuations in the Middle Permian of China. *Science*, 324(5931): 1179–1182.
- Wu Libin, Liu Xiaodong and Xu Liqiang, 2017. Change of

- organic  $\delta^{13}\text{C}$  in Ormithogenic sediments of the Xisha Archipelago, South China Sea and its implication for ecological development. *Acta Geologica Sinica* (English Edition), 91(3): 1109–1119.
- Wu Xiaoqi, Liu Quanyou, Liu Guangxiang, Wang Ping, Li Huaji, Meng Qingqiang, Chen Yingbin and Zeng Huasheng, 2017. Geochemical characteristics and genetic types of natural gas in the Xinchang Gas Field, Sichuan Basin, SW China. *Acta Geologica Sinica* (English Edition), 91(6): 2200–2213.
- Xiao Sheng, Xiao Chuantao and Liang Wenjun, 2015. Carbon and oxygen isotope composition of carbonatic rock from the Middle Permian–Lower Triassic in Chuanxi Area. *Science & Technology Review*, 33(22): 19–26 (in Chinese with English abstract).
- Xu Yigang, He Bin, Huang Xiaolong, Luo Zhenyu, Zhu Dan, Ma Jinlong and Shao Hui, 2007. Late Permian Emeishan flood basalts in Southwestern China. *Earth Science Frontiers* (English Edition), 14(2): 1–9.
- Xu Yigang, He Bin, Luo Zhenyu and Liu Haiquan, 2013. Study on mantle plume and large igneous provinces in China: an overview and perspectives. *Bulletin of Mineralogy Petrology & Geochemistry*, 32(1): 25–39 (in Chinese with English abstract).
- Xu Yigang, Zhong Yuting, Wei Xun, Chen Jun, Liu Haiquan, Xie Wei, Luo Zhenyu, Li Hongyan, He Bin, Huang Xiaolong, Wang Yan and Chen Yun, 2017. Permian mantle plumes and earth's surface system evolution. *Bulletin of Mineralogy, Petrology and Geochemistry*, 36(3): 359–373 (in Chinese with English abstract).
- Xu, Y.G., He, B., Chung, S.L., Menzies, M.A., and Frey, F.A., 2004. Geologic, geochemical, and geophysical consequences of plume involvement in the Emeishan flood–basalt province. *Geology*, 32(10): 917–920.
- Xu, Y.G., Luo, Z.Y., Huang, X.L., He, B., Xiao, L., Xie, L.W., and Shi, Y.R., 2008. Zircon U–Pb and Hf isotope constraints on crustal melting associated with the Emeishan mantle plume. *Geochimica Et Cosmochimica Acta*, 72(13): 3084–3104.
- Xue Wuqiang, Li Bo, Yan Jiabin, Brooks B. Ellwood, Jonathan H. Tomkin, Wang Yan and Zhu Zongmin, 2015. High-resolution floating point time scale (FPTS) of Permian Capitanian stage in South China. *Chinese Journal of Geophysics*, 58(10): 3719–3734 (in Chinese with English abstract).
- Yan Zhaobin, Guo Fusheng, Pan Jiayong, Guo Guolin and Zhang Yuejing, 2005. Application of C, O and Sr isotope composition of carbonates in the research of paleoclimate and paleo–oceanic environment. *Contributions to Geology and Mineral Resources Research*, 20(1): 53–65 (in Chinese with English abstract).
- Yang Yuqing and Feng Zengzhao, 2000. Permian deposition system in South China. *Journal of Palaeogeography*, 2(1): 11–18 (in Chinese with English abstract).
- Yang Zhengyu, Shen Weizhou and Zheng Liandi, 2009. Elements and isotopic geochemistry of Guadalupian–Lopingian boundary profile at the Penglaitan Section of Laibin, Guangxi province, and its geological implications. *Acta Geologica Sinica*, 83(1): 1–15 (in Chinese with English abstract).
- Yin Hongfu and Song Haijun, 2013. Mass extinction and Pangea integration during the Paleozoic–Mesozoic transition. *Science China: Earth Sciences*, 56(11): 1791–1803.
- Zeng, J., Cao, C.Q., Davydov, V.I., and Shen, S.Z., 2012. Carbon isotope chemostratigraphy and implications of Palaeoclimatic changes during the Cisuralian (Early Permian) in the Southern Urals, Russia. *Gondwana Research*, 21(2–3): 601–610.
- Zhang Liqin, 2013. Palaeoenvironmental change across the Guadalupian–Wuchiapingian boundary in Sichuan, South China. *Acta Geologica Sinica* (English Edition), 87 (Suppl.1): 880–882.
- Zhang Zhaochong, John J Mahoney, Wang Fusheng, Zhao Li, Ai Yu and Yang Tiezheng, 2006. Geochemistry of picritic and associated basalt flows of the western Emeishan flood basalt province, China: evidence for a plume–head origin. *Acta Petrologica Sinica*, 22(6): 1538–1552 (in Chinese with English abstract).
- Zhang, H., Cao, C.Q., Liu, X.L., Mu, L., Zheng, Q.F., Liu, F., Xiang, L., Liu, L.J., and Shen, S.Z., 2015. The terrestrial end–Permian mass extinction in South China. *Palaeogeography, Palaeoclimatology, Palaeoecology*, 448: 108–124.
- Zhong, Y.T., He, B., Mundil, R., and Xu, Y.G., 2014. CA–TIMS zircon U–Pb dating of felsic ignimbrite from the Binchuan section: implications for the termination age of Emeishan large igneous province. *Lithos*, 204(3): 14–19.
- Zhou Yexin, Ding Jun, Yu Qian, Wang Jian, Men Yupeng, Xiong Guoqing, Xiong Xiaohui and Deng Qi, 2017. Sedimentary and organic carbon isotopic characteristics of Kuanyinchiao Member in Northeastern Chongqing and its regional correlation. *Acta Geologica Sinica*, 91(5): 1097–1107 (in Chinese with English abstract).
- Zhou, M.F., Malpas, J., Song, X.Y., Robinson, P.T., Sun, M., Kennedy, A.K., Leshner, C.M., and Keays, R.R., 2002. A temporal link between the Emeishan large igneous province (SW China) and the end–Guadalupian mass extinction. *Earth & Planetary Science Letters*, 196(3): 113–122.
- Zhu Jingquan, Li Yongtie, Jiang Maosheng and Chen Daizhao, 2004. Carbon isotope composition and its implications of lower Cretaceous Aptian–Albian shallow water carbonates in the Cuoqin Basin, North Tibet. *Science in China* (Series. D), 47(3): 247–254.

#### About the first author

QU Hongjun, male; born in 1967 in Baoji city, Shaanxi province; He is now a professor in Department of Geology, Northwest University of China. His research interests are sedimentology and petroleum geology. E-mail: hongjun@nwu.edu.cn.; phone: 13772500178.